RESEARCH PAPER

Anisotropy of Fractal Dimensions of Fractures and Loading Curves of Steel Samples During Impact Bending

V. Usov[1*], M. Rabkina[2], N. Shkatulyak[1], E. Savchuk[1] and O. Shtofel[2]

** valentinusov67@gmail.com*

Received: January 2020 Revised: May 2020 Accepted: October 2020

[1] South Ukrainian National Pedagogical University named after K. D. Ushinsky, Department of Technological and Professional Education, Odessa, Ukraine

[2] The E. O. Paton Electric Welding Institute NAS of Ukraine, Kiev, Ukraine

DOI: 10.22068/ijmse.17.4.142

Abstract: *This study aims to establish the correlation between the impact strength and texture, fractal dimensions of fractures (D_f), fractal dimensions (D_C) obtained from load-time diagrams P(τ) reflecting the applied load (P) dependence on time (τ) during the Charpy impact test of 20K steel at various temperatures as well as the comparison of the abovementioned fractal dimensions. The tests were carried out on a vertical impact testing machine with a multi-channel system for high-speed registration of forces and strains, as well as a heating and cooling system for samples in a wide temperature range. The load vs. time (load dependence on time) diagrams were obtained at an impact velocity of V_0 = 4.4 m/s at temperatures of -50, +20, + 50℃. The Charpy standard samples of 20K steel (analog to DIN17175, class St45.8) were cut in various directions out of a 12 mm thick the destroyed tank shell of a distillation column for oil refining. It was established that the behavior of both the abovementioned fractal dimensions depending on the cutting direction and test temperature coincides qualitatively. The trend of decreasing in fractal dimension with a more viscous nature of fracture was found. The effect of texture is discussed.*

Keywords: *impact tests, diagram of load changes depending on time, impact toughness, fractal dimension, texture.*

1. INTRODUCTION

The Charpy impact tests allow finding the characteristics which are important for structural materials, such as impact strength, brittle-ductile transition temperature, that is, the temperature at which the fracture of the material during loading changes from viscous to brittle. The above data are essential for predicting the safe operation of the designed structures. The ductile-brittle transition temperature (DBTT) using Charpy instrumental tests can be determined by various methods. Among them, there can be, for example, the lateral expansion, the appearance of shear fracture, the average value of impact strength, the use of a load diagram, a master curve [1]. To assess the resistance to brittle fracture of structural materials, in particular steel, impact tests (KCV) of a series of Charpy samples are usually carried out at various temperatures. At this method, the study of fracture surfaces is a very important process, because it allows you to get an additional estimate of the temperature of the plastic-brittle transition. The critical temperature for the transition of a material from a viscous state to a brittle one (T_{br}) is determined from the graphical impact strength dependence on temperature. One of the methods for determining the critical temperature of brittleness is based on the fact that the proportion of brittle and viscous component is in the ratio “50:50” at this temperature [2-4].

A significant scatter of the obtained data takes place at using various equipment for impact testing and different assessment methods [5-7].

The texture of polycrystalline bodies is the main cause of the anisotropy of their physical and mechanical properties. Therefore, the presence of texture in the material is also one of the reasons for this scattering [8-10]. Regarding this, it is also necessary to take into account the cutting direction of samples from sheets or tubular fragments of the study materials for physical research and mechanical testing.

The use of modern techniques and high-speed systems for recording diagrams, which reflect the applied load dependence on the fracture time, makes it possible to increase the informational content of impact strength tests [11-13].

Additional information can also be obtained by studying the relationship between the impact

[DOI: 10.22068/ijmse.17.4.142]

toughness and fractal dimension (FD) of the fractures [14, 15].

It should be noted that the description of fracture surfaces in the language of fractals and the correlation connection with the FD index and the mechanical properties of materials have still been being debated [16].

It should be noted that the description of fracture surfaces in the language of fractals and the correlation connection the FD index and the mechanical properties of materials have still been being debated [16]. So, for example, in [17, 18], the correlation between the crack fractal dimension, the value of the stress intensity factor, and the structure of the pre-fracture zone with an invariant complex of mechanical properties are indicated. The correlation connection with the fractal dimension of fractures and the durability of the tested samples is traced in [14]. As durability decreases, the value of the fractal dimension increases. It is shown that the FD increases with increasing the number of cycles to failure. In [19] and several other earlier studies, an extensive review of which is also presented in [19], it was shown that ductile alloys show a decrease in fractal dimension with increasing viscosity, while brittle alloys demonstrate the opposite behavior.

However, not all studies using impact toughness are concordant. In [20], it is questioned that a fracture is a self-similar object in the case of viscous fracture.

This study aims to establish the correlation (correlative values) between the impact toughness and the texture, fractal dimension (D_f) of fractures, fractal dimensions (D_C) determined from load-time diagrams $P(\tau)$ reflecting the applied load (P) dependence on time (τ) during the Charpy impact test of 20K steel at various temperatures as well as the comparison of the abovementioned fractal dimensions.

2. EXPERIMENTAL PROCEDURE

The material for the study was a fragment of steel 20K (analog to DIN17175, class St45.8), cut out of the destroyed tank shell of a distillation column for oil refining. The diameter of the tank shell was 2200 mm including wall thickness of 12 mm. The chemical composition of steel: 0.19 % C; 0.27 % Si; 0.65 % Mn; 0.2 % Cu; 0.23 % Ni; 0.23% Cr; 0.25 % As; 0.05 % S; 0.035% P; Fe is balance in mass percent. Three groups of the Charpy standard samples cut in different directions out of the abovementioned steel fragment were used to study the anisotropy of the impact toughness. The first group of samples was cut along the longitudinal direction (LD), the second group was cut perpendicular to the longitudinal direction, i.e. in the transverse direction (TD), and the third group - at an angle of 45˚ to RD, i.e. in the diagonal direction (DD), as shown in Fig. 1. The Charpy standard samples with a V-shaped notch had dimension (55×10×10) mm.

Impact tests were carried out[1] by an impact tension machine, equipped with a multichannel system for recording forces and strains, as well as a system for heating and cooling samples in a wide temperature range [21, 22]. The impact velocity V_0 was 4.4 m/s.

The high sensitivity of the recording system allows us to divide the load diagram into characteristic areas and calculate the values of the total deformation and fracture energy and its components: crack initiation energy, viscous crack growth energy, brittle crack penetration energy, and viscous crushing energy [22].

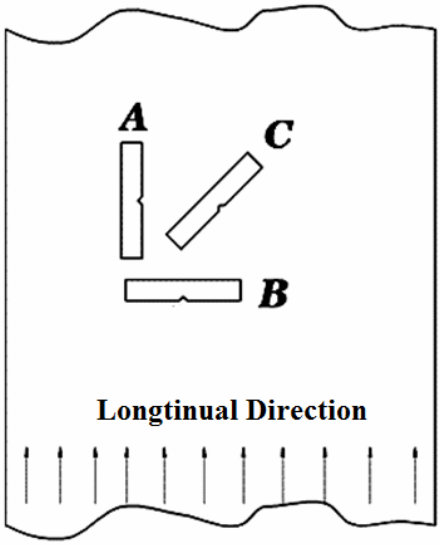

Fig. 1. Scheme of specimens cutting out of the tubular fragment of the steel 20K by length of 2200 mm and thickness of 12 mm for impact tests

The specific fracture energy W_{sp} (KCV) was determined by the formula [23]:

$$W_{sp}=W/S_0 \quad (1)$$

[1] Tests were carried out by Kondryakov E.A.

[DOI: 10.22068/ijmse.17.4.142]

Where W is the energy of destruction, S_0 is the original cross-sectional area of the sample in the place of the stress concentrator, m^2, which calculated by the formula [23]

$$S_0=H_1B \quad (2)$$

Where H_1 is the original height of the sample's working part, m;
B is the original width of the sample, m. The B and H_1 values are measured with an error that is not more than ± 0.05 mm [23].
The JSM-840 scanning electron microscope in the secondary (SEI) electron mode at an accelerating voltage of 20 kV and magnifications ×10 ... ×1000 was used to study the morphology of fractures.

X-ray method by means of inverses pole figures (IPFs) was used for studying the texture. We carried out the θ-2θ scanning by the DRON-3 m diffractometer by the Bragg-Brentano geometry of investigated samples in the plane perpendicular to the normal direction (ND) to the steel surface and in the plane perpendicular to the longitudinal direction (LD). The sample without the texture (standard) was also scanned under identical geometric conditions. The standard sample was made of fine sawdust after its recrystallization during the vacuum annealing for 1 hour at 450 ˚C. The Morris normalization was used at the IPFs construction [24].
The fractal dimension D was determined by the box method. An illustration of this method is shown in Fig. 2.

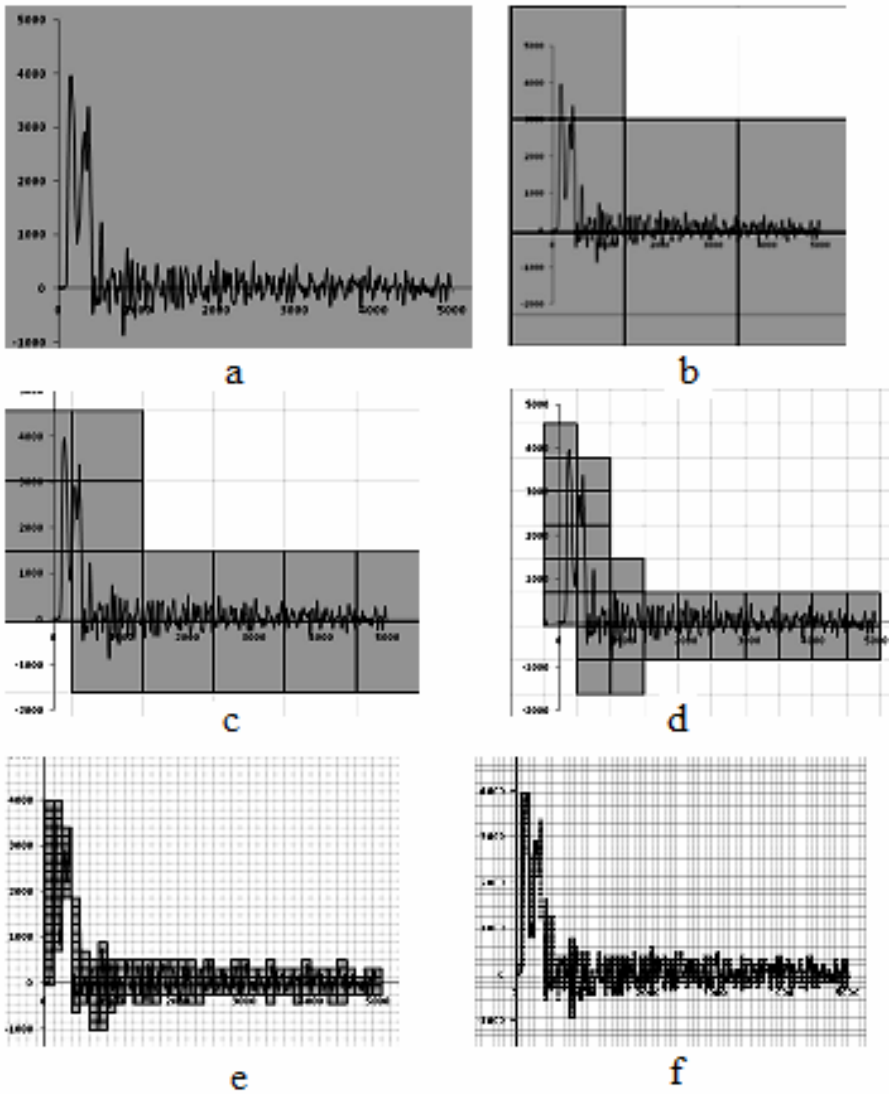

Fig. 2. Illustration of using the method of cells (box method) to the curve fractal dimension determination

[DOI: 10.22068/ijmse.17.4.142]

The essence of this method is that to determine the fractal dimension it's necessary to cover the image of a curved profile or a selected fracture fragment border with elementary square grids with sides of l_i [25]. At each stage of this method application, the same curve is covered with cells of a reduced scale. The smaller the cell size, the more accurately the curve is reproduced. At the same time, we count the number of squares N (l_1) that the curve intersects. Then we change the size of the grid window ℓ_i. Again we count the number of squares that were crossed by the curve: $N(l_2)$, $N(l_3)$, ..., $N(l_n)$. The number of squares $N(l_i)$, which were crossed by the curve is connected with the size of the grid window l_i by the formula [25]:

$$N(l)=\lim_{l\to 0}\alpha.l^{-D} \quad (3)$$

Where $D=\lim_{l\to 0}\frac{\ln N(l)}{\ln(1/l)}$ by definition, is usually called the fractal dimension or the Hausdorff-Besikovitch dimension [25].

Practically D is found by the tangent of angle slope of the graphical dependence $lgN(l_i)=f(lgl_i)$ [25].

To determine the fractal dimension, HarFA (Harmonic and Fractal Image Analysis) computer software was used [26] (Fig. 3).

Before determining the fractal dimension, the fracture photographs were cleaned from noise using the ACDSee Photo Studio Software [27], to obtain only the boundary lines of the fracture fragments (Fig. 3).

3. RESULTS AND DISCUSSION

In the studied fragment of 20K steel takes place the impact toughness anisotropy (Table 1). Samples cut out in the longitudinal direction (LD), have the least resistance to destruction. Samples cut out in the transverse direction (TD) have the maximum value of the impact toughness. Samples, cut out at an angle of 45° to the LD (i.e. in the DD) have the intermediate value of the impact toughness but the difference between the two latter is minor.

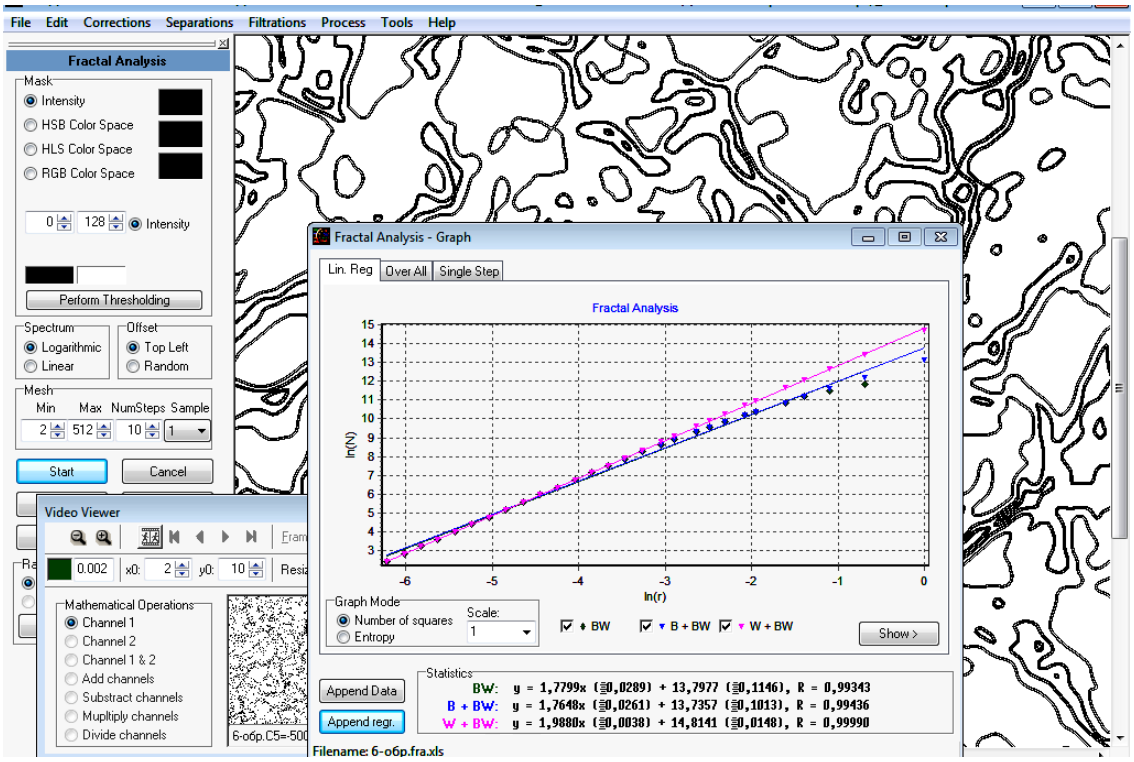

Fig. 3. An example of using the Harfa computer program.

[DOI: 10.22068/ijmse.17.4.142]

Table 1. The specific fracture energy W_{sp}, J/m^2, at the impact tests.

Specimen, №	-50°C	+20°C	+50°C
Longitudinal Direction LD			
1	0.83	5.04	22.87
2	0.73	4.31	20.82
Average value	0.78	4.67	21.84
Transverse direction TD			
1	0.97	9.88	47.95
2	0.95	10.91	57.95
Average value	0.96	10.39	52.95
Diagonal direction DD (LD+45º)			
1	0.85	13.33	47.24
2	0.91	17.70	54.65
Average value	0.88	15.51	50.94

Micrographs of fractures are shown in Figures 4, 5. Preliminary analysis of presented micrograms was carried out with a slight increase to determine the general nature of the destruction (Fig. 4). This made it possible to accurately determine the position of the areas of brittle and viscous destruction, as well as the beginning of destruction. As is well known, the energy of the nucleation of destruction, all other conditions being the same, is determined by the temperature and the microstructure nature. The destruction under the notch basically begins as viscous even at negative temperatures due to the peculiarities of the complex-stressed state at the top of the notch (Fig. 4). As can be seen, fractures in this zone have ductile elements of the destruction (bridges and individual viscous pits) as well as deep secondary cracks running from the notch and crossing the entire surface of the fracture, down to the rupture (Fig. 4).

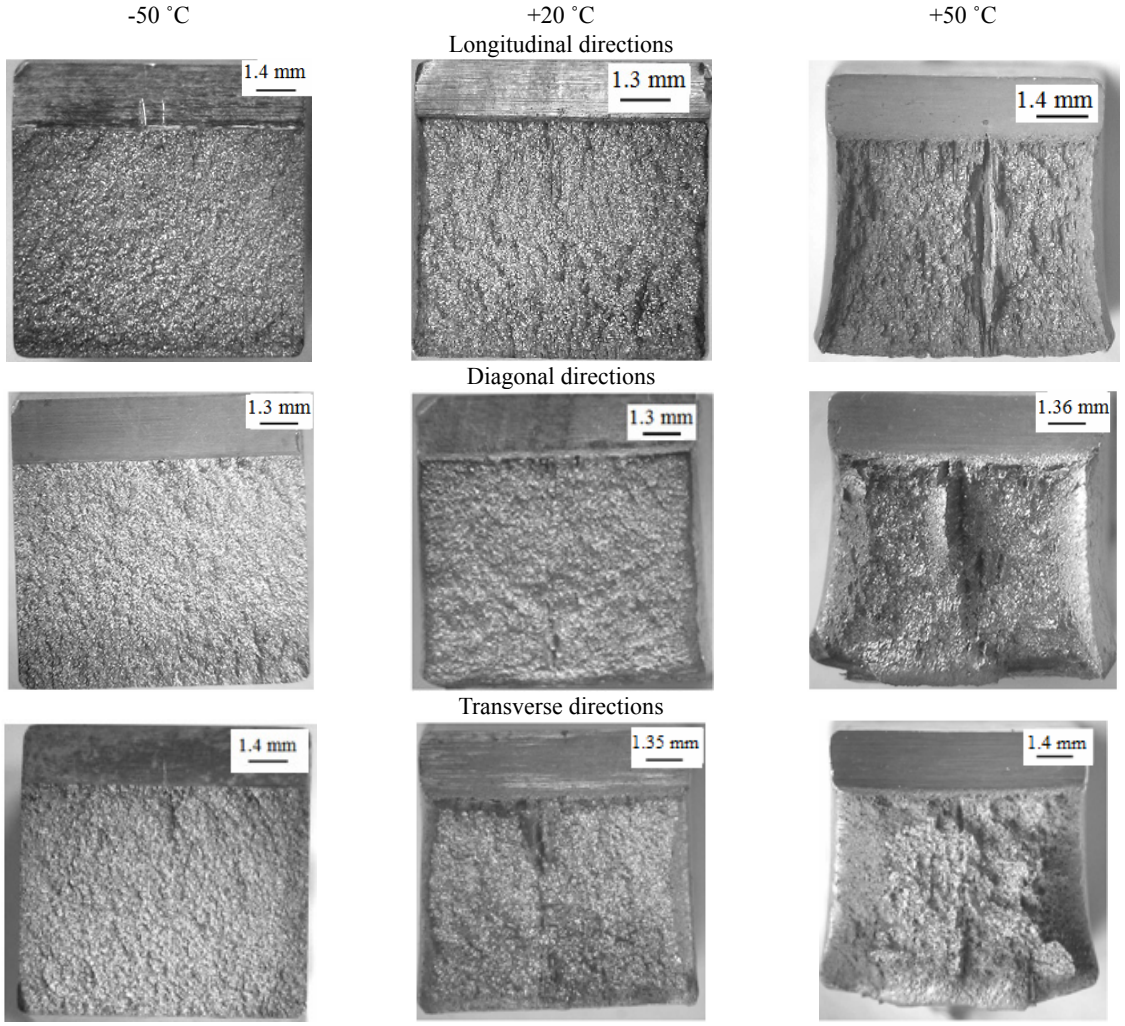

Fig. 4. SEM photography of fractures surfaces after impact tests at various temperatures of 20K steel samples cut in the longitudinal, diagonal and transverse directions.

[DOI: 10.22068/ijmse.17.4.142]

Secondary cracks are most pronounced in the sample cut out in the LD (Fig. 4, c, f). The formation of such cracks in the fracture indicates the presence in the metal of the texture, which determines the resistance to viscous fracture (Table 1).

The metal is destroyed by the mechanism of quasi-cleavage in the whole range of tests temperatures in all directions as further studies have shown (Fig. 5).

Facets of quasi-cleavage have sizes 10 ... 40 microns. The fraction of the viscous component in quasi-cleavage increases with an increase of the test temperature.

Fig. 6 shows the diagrams dependencies of the applied force P on the time τ in the process of impact tests at different temperatures of specimens cut out in various directions from the fragment of 20K steel.

Magnitudes of fractures fractal dimensions D_f of studied samples, as well as the fractal dimensions of diagrams, P(τ) are presented in tables 2, 3. Fractal dimensions of both D_f and D_c have minimal values at elevated temperature of tests + 50 ˚C (tables 2, 3).

At the same time, the impact toughness at test temperature + 50 ˚C is maximal (Table 1). This indicates the viscous nature of the destruction at + 50 ˚C. Maximal values of D_f and D_c take place at a low test temperature of -50 ˚C (tables 2, 3). At the same temperature, the minimal value of impact toughness takes place (table 1), which corresponds to the brittle character of the destruction of study samples at the -50 ˚C.

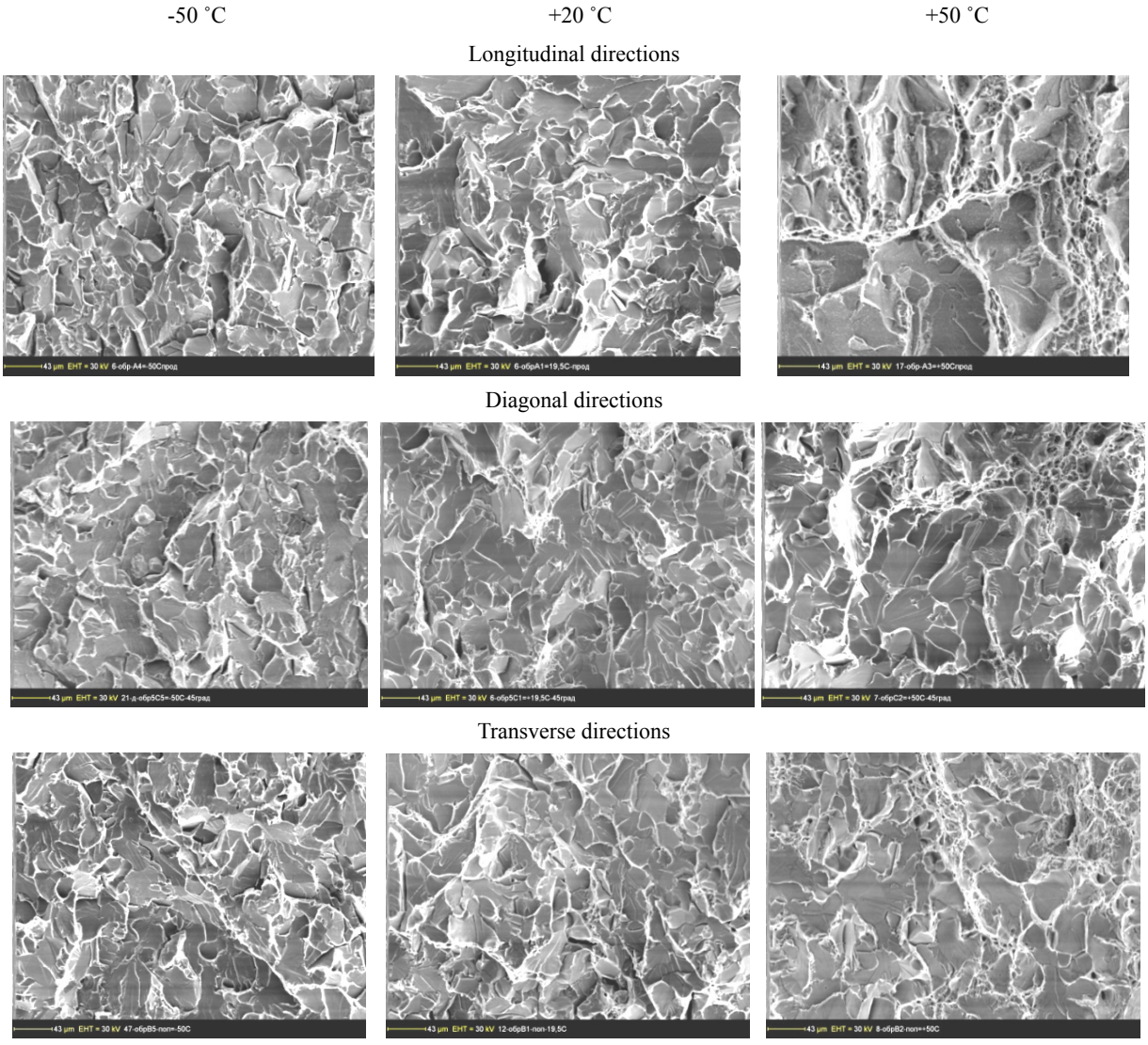

Fig. 5. SEM photographs of fractures surfaces after impact tests at various temperatures of 20K steel samples cut in the longitudinal, diagonal and transverse directions.

[DOI: 10.22068/ijmse.17.4.142]

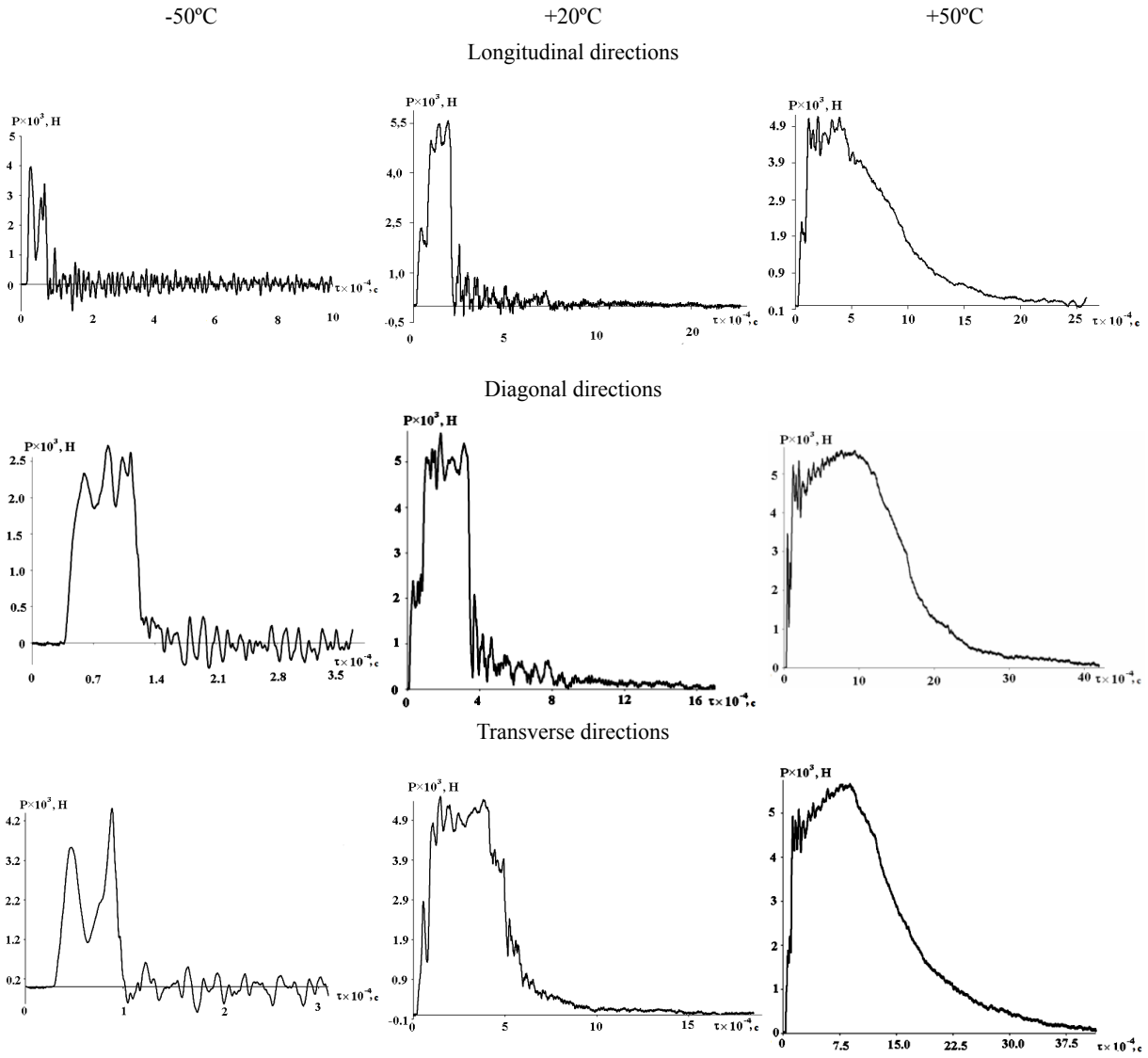

Fig. 6. Diagrams of the applied load (P) from time (τ) during impact test at various temperatures of 20K steel samples cut in the longitudinal, diagonal and transverse directions.

Table 2. The fractal dimension (D_f) of the fractures shown in Figure 5

t,˚C	LD	TD	DD	Average D_f
-50	1.59±0.01	1.60±0.01	1.64±0.01	1.61±0.01
+20	1.55±0.01	1.56±0.01	1.59±0.01	1.57±0.01
+50	1.52±0.01	1.54±0.01	1.55±0.01	1.54±0.01

Table 3. The fractal dimension (D_c) of the P(τ) diagrams shown in Figure 7

T, ˚C	RD	TD	DD	Average D_c
-50	1.27±0.01	1.23±0.01	1.31±0.01	1.27±0.01
+20	1.23±0.01	1.17±0.01	1.26±0.01	1.22±0.01
+50	1.12±0.01	1.13±0.01	1.16±0.01	1.14±0.01

With increasing fracture toughness (table 1), the fractal dimension of the fracture surface decreases (tables 2 and 3). Similar results were obtained in [19]. In particular, at testing a series of 24 samples of AISI 4340 steel, it was shown that the fractal dimension of the fracture surface

[DOI: 10.22068/ijmse.17.4.142]

decreased from 1.28 to 1.10-1.09 with increasing the viscous component in the crack from 36 to 100 % [19]. Decreasing fractal dimension with a more viscous nature of fracture can be explained by the fact that the surface is more "elongated" because of the presence of wider and deeper microcavities. At the microscopic level, the surface becomes smoother.

Maximum values of the fractal dimension, for both D_f and, D_c are observed for samples cut out in the diagonal direction (DD), i.e. the fractal dimension anisotropy takes place (tables 2 and 3). This anisotropy can be caused by texture.

Experimental IPFs of the 20K steel are presented in Fig. 7. The main texture component of the studied steel is {001} <110>, as you can see in Fig. 7. This component is typical for the rolling texture of BCC steels [28]. In this case, the {001} crystallographic planes, which are brittle cleavage planes in BCC metals [29], are located perpendicular to the diagonal direction. Cleaving can occur along this crystallographic plane that promotes the more brittle nature of the destruction in diagonal specimens and is manifested in increasing their fractal dimension.

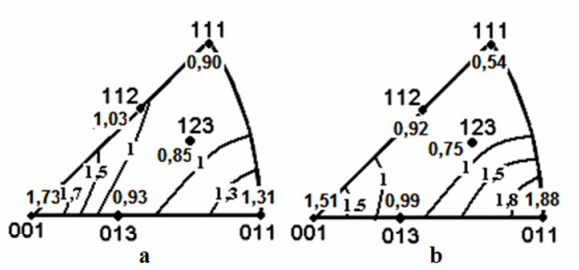

Fig. 7. IPFs of the investigated 20K steel: a) ND; b) LD

4. CONCLUSION

1. Impact toughness values KCV have defined on standard Charpy specimens cut in different directions out of a tubular fragment of Steel 20K (analog to DIN17175, class St45.8) with a thickness of 12 mm. Tests diagrams P(τ) reflecting the applied load (P) dependence on time (τ) are presented. Fractal dimensions (D_c) of diagrams P(τ) and fractal dimensions of fractures (D_f) are compared after impact tests in the temperature range from -50 ˚C up to + 50 ˚C.
2. Maximum average values of both fractals dimensions D_f and D_c correspond to the brittle character of the destruction and minimum impact toughness.
3. Minimum average values of both fractals dimensions D_f and D_c corresponds to the viscous character of destruction and maximum impact toughness.
4. The largest values of the fractal dimension found for specimens cut out at an angle of 45˚ to the longitudinal direction are induced by the {001} <110> texture component, which is the main texture component of low alloy steels with a BCC lattice.
5. Presented results can be used to estimate the steel tendency to brittle fracture by analyzing the fracture energy and fractal dimension of the load dependence on time diagrams at impact toughness tests.

REFERENCES

1. Standard Test Methods for Notched Bar Impact Testing of Metallic Material, https://mmplab.um.ac.ir/images/248/standard/impact/E23_12c_Standard_Test_Methods_for.pdf
2. Cubides-Herrera C.S.; Villalba-Rondón D.A.; Rodríguez-Baracaldo R. "Charpy impact toughness and transition temperature in ferrite – perlite steel", Scientia et Technica Año XXIV, 2019, 24 (2), 200-204.
3. Zhao Y.J., Su Y.M., Liu M., Hu Z.L., and Tang P. "Ductile-to-brittle transition and impact fracture behavior of 3Mn–Si–Ni low carbon martensitic steel", Strength of Materials, 2019, 51, 2, 291-299.
4. Khlybov A.A., Kabaldin Yu.G., Anosov M.S., Ryabov D.A., Naumov V.I. and Sentyureva V.I. "The effect of low temperatures on the operability of products 20GL steel". Journal of Physics: Conference Series, 2020, 1431, 012063.
5. Orynyak I., Zarazovskii M., Bogdan A. "Determination of the transition temperature scatter using the Charpy data scatter", Proceedings of the ASME 2013 Pressure Vessels and Piping Conference PVP2013 July 14-18, 2013, Paris, France PVP2013-97697.
6. Takashima Ya., Ohata M. and Minami F. "Analysis of Statistical Scatter in Charpy Impact Toughness", Materials Science Forum, 2014, 783-786, 2394-2399.

[DOI: 10.22068/ijmse.17.4.142]

7. Mohr W., "Scatter in Charpy Data Considered as a Transferrable Parameter", EWI, https://ewi.org/wp-content/uploads/2019/08/ Mohr-Scatter-in-Charpy-Data-FINAL.pdf
8. Inagaki H., Kurihara K. and Kozasu I. "Influence of Crystallographic Texture on the Strength and Toughness of Control-rolled High Tensile Strength Steel", Transactions ISIJ, 1977, 17, 75-81.
9. Petrov R., Garcìa O.L., Mulders J.J.L., Reis A.C.C., Bae J.-H., Kestens L. and Houbaert Y. "Three Dimensional Microstructure–Microtexture Characterization of Pipeline Steel", Materials Science Forum, 2007, 550, 625-630.
10. Chao J. and Capdevila C. "The Influence of Texture on the Ductile-to-Brittle Transition Behavior in $Fe_{20}Cr_{4.5}Al$ Oxide Dispersion Strengthened Alloy", Metals, 2020, 10(1), 87.
11. Sahraoui S., El Mahi A., Castagnede B. "Measurement of the dynamic fracture toughness with notched PMMA specimen under impact loading", Polymer Testing, 2009, 28(7), 780-783.
12. Kravchyk A., Kondryakov E. "Study of rolling direction influence on deformation and fracture energy of the charpy specimens". Visnyk NTUU "KPI" Seriya mashinobuduvannya, 2016, 2, (77), 89-93.
13. Pan J., Chen Z., Hong Z. "A novel method to estimate the fracture toughness of pressure vessel ferritic steels in the ductile to brittle transition region using finite element analysis and Master Curve method", International Journal of Pressure Vessels and Piping, 2019, 176: 103949.
14. Usov V.V., Gopkalo E.E., Shkatulyak N.M. et al., "Texture, microstructure, and fractal features of the low-cycle fatigue failure of the metal in pipeline welded joints", Russian Metallurgy (Metally), 2015, 9, 759-770.
15. Liang J.-Z. "Relationship between fractal dimensions of fracture surface and impact toughness of polycaprolactone/nano-CaCO3 composites", Adv Polym Technol., 2018, 37, 3115–3122.
16. Lucas Máximo Alves "Foundations of Measurement Fractal Theory for the Fracture Mechanics", 2012, In book: Applied Fracture Mechanics, Intech-Open, Editors: Alexander Belov, doi:10.5772/51813
17. Ivanova, V.S., Bunin, I.J. & Nosenko, V.I. "Fractal material science: A new direction in materials science", JOM, 1998, 50, 52–54.
18. Schelokova M.A., Slobodian S.B., Dyrda V.I. "Fractal approach to solid fracture mechanics", Geo-technical mechanics, 2018, 138, 227-259.
19. Carney L.R., Mecholsky J.J. "Relationship between Fracture Toughness and Fracture Surface Fractal Dimension in AISI 4340 Steel", Materials Sciences and Applications, 2013, 4, 258-267.
20. Santos, S.F.D., Rodrigues, J.D.A. **"**Correlation between fracture toughness, work of fracture and fractal dimensions of Alumina-mullite-zirconia composites**"**, Materials Research, 2003,6 (2) 219-226.
21. Kondryakov E. A., Zhmaka V. N., Kharchenko V. V., "The system for measuring deformations and forces during dynamic testing of materials", Problems of Strength, 2005, 3, 140-145 [in Ukrainian].
22. Kharchenko V. V., Kondryakov E.A., Zhmaka V.N. et al., "Effects of temperature and loading rate on the energy of crack initiation and propagation in the Charpy specimens from carbon steels", Problems of Strength, 2006, 5, 120-127.
23. "GOST 9454 78 format for editing. Metals shock test method at low, room and high temperatures metals" Danilov V., Georgiev M., Mezhova N., Kosarev L., Komolova E., Drozdovsky B., Kudryashov V., Odessa P., Helmida V., Zmievsky V., https://polipharm.ru/en/kredity/gost-9454-78-format-dlya-red aktirovaniya-metally-metod-ispytaniya-na/
24. Stoica G.M., Stoica A.D., An K., Ma D., Wang X.-L. "Extracting Grain-Orientation Dependent Data from In-Situ Time-of-Flight Neutron Diffraction– I. Inverse Pole Figures", J. Appl. Cryst., 2014, 47, 2019–2029.
25. Rajković N., Krstonošić B. and Milošević N. "Counting Method of 2D Neuronal Image: Method Modification and Quantitative Analysis Demonstrated on Images from the Monkey and Human Brain", Hindawi Computational and Mathematical Methods in Medicine, https://doi.org/10.1155/2017/ 8967902
26. "HarFA, Harmonic and Fractal Image Analyser, Software For Determination of Fractal Dimension", 2001, Zmeskal, O, Bzatek, T, Nezadal, M, and Buchnicek, M, www.fch.vutbr.cz/lectures/imagesci

[DOI: 10.22068/ijmse.17.4.142]

27. "ACDSee Photo Studio Professional 2019-Built for Professionals", https://acdsee-pro.software.informer.com/2019.1/
28. "Lobanov M., Danilov S., Pastukhov V., Pyshmintsev I., and Urtsev V. "Effect of Structure and Textureon Failure of Pipe Steel Sheets produced by TMCP" in XIX International scientific-technical conference "The Ural school-seminar of metal scientists-young researchers", KnE Engineering, 2019, 121–127, DOI 10.18502/keg.v1i1.4399, https://knepublishing.com/index.php/KnE-Engineering/article/view/4399/9024
29. Pineau A., Benzerga A.A. Pardoen T. "Failure of metals I: Brittle and ductile fracture", Acta Materialia, 2016, 107, 424-483.

[DOI: 10.22068/ijmse.17.4.142]